Nanoscale Horizons

Understanding the Effects of Adduct Functionalization on C60 Nanocages for the Hydrogen Evolution Reaction

Journal:	*Nanoscale Horizons*
Manuscript ID	NH-COM-11-2024-000586.R1
Article Type:	Communication
Date Submitted by the Author:	07-Jan-2025
Complete List of Authors:	Spears, Joy; Hampton University Shawky, Mina; Mansoura University, chemistry Castro, Edison; The University of Texas at El Paso Puente Santiago, Alain; Florida International University, Chemistry and Biochemistry Echegoyen, Luis; University of Texas at El Paso, Department of Chemistry He, Tianwei; Yunnan University, Dares, Christopher; Florida International University, Chemistry and Biochemistry Noufal, Mohamed ; Hampton University

New concepts

In this work, we thoroughly investigated the electrocatalytic performance of two pyridyl-pyrrolidine functionalized C_{60} fullerenes for the hydrogen evolution reaction (HER) using advanced experimental and theoretical tools. These functionalized fullerenes showed an exceptional electron density relocation at the C_{60}-ligand interfaces, which significantly impacts the electronic structure of the carbon atoms in the nearest regions, thus inducing a new type of highly active electrocatalytic sites for the molecular generation of hydrogen. Notably, the mono-(pyridyl-pyrrolidine) penta-adduct of C_{60} has exhibited a remarkable HER catalytic activity as a metal-free catalyst, delivering an overpotential (η_{10}) of 75 mV vs. RHE and a very low onset potential of -45 mV vs. RHE. Additionally, we identified the key factors that influence the intermolecular electron transfer at the C_{60}-addend interface and their impact on the HER. This work introduces new chemistry concepts to understand the origin of the electrocatalytic activity of metal-free 0D-low-dimensional nanomaterials with curved surfaces.

Understanding the Effects of Adduct Functionalization on C_{60} Nanocages for the Hydrogen Evolution Reaction

Joy Spears,[1] Mina Shawky Adly,[2] Edison Castro,[3] Alain R. Puente Santiago,[4*] Luis Echegoyen,[3] Tianwei He,[5*] Christopher J. Dares,[4] and Mohamed Noufal[1*]

[1]Department of Chemical Engineering, Hampton University, Hampton, VA 23668, USA.

[2]Deparment of Chemistry, Faculty of Science, Mansoura University, Al-Mansoura 35516, Egypt.

[3] Department of Chemistry, University of Texas at El Paso, 500 West University Avenue, El Paso, Texas 79968, United States

[4] Florida International University (FIU), Department of Chemistry and Biochemistry, Miami, FL, USA.

[5]National Center for International Research on Photoelectric and Energy Materials, Yunnan Key Laboratory for Micro/Nano Materials& Technology, School of Materials and Energy, Institute of International Rivers and Eco-Security, Yunnan University, Kunming 650091, China

KEYWORDS: Low-dimensional materials, 0D-Fullerenes, Functionalized fullerenes, Bis-pyrrolidine hexa-adducts of $C_{60,}$ HER

ABSTRACT: In this work, we use experimental and theoretical techniques to study the origin of the boosted hydrogen evolution reaction (HER) catalytic activity of two pyridyl-pyrrolidine functionalized C_{60} fullerenes. Notably, the mono-(pyridyl-pyrrolidine) penta-adduct of C_{60} has exhibited a remarkable HER catalytic activity as a metal-free catalyst, delivering an overpotential (η_{10}) of 75 mV vs. RHE and a very low onset potential of -45 mV vs. RHE. This work addresses fundamental questions about how functionalization on C_{60} changes the electron density on fullerene cages for high-performance HER electrocatalysis.

The HER must achieve technological maturity, relying on widely available carbon-based materials. Pt-group metal (PGM) catalysts constitute a significant portion of the design and cost for proton-exchange membrane fuel cells (PEMFCs) and electrolyzers.[1-3] Over the past decade, substantial efforts have been made to develop PGM-free cathodes for HER, especially with the recent promising developments in metal-N-C-based and metal single-atom alternatives to PGMs.[4] Most recent reports have focused on studies of metal-containing carbides and Ni-based materials for HER catalysis, which exhibit only moderate activities and require greater stability and reproducibility.[4-6] Low-dimensional carbons, such as 1D-carbon nanotubes and 2D-graphene, have been used as metal-free catalysts for the electrochemical generation of molecular hydrogen because of their large surface area, excellent chemical stability, and high conductivity.[7, 8] Despite these advances, employing metal-free catalysts for HER and their applications remains challenging due to their large molecular footprint, poor durability, and limited electrochemical stability.[9, 10] With the latest progress in electrocatalysts, properties such as high electrochemical stability and high conductivity, are drawing researchers to use molecular catalysts for energy conversion applications.[11] 0D-based fullerene architectures have recently emerged as a unique alternative to reduce protons to hydrogen molecules for fuel cell applications.[12-16] The distinctive chemical and physical characteristics of fullerenes and their derivatives primarily arise from their electron-accepting abilities and high charge transport capabilities in three dimensions. However, the role of interfacial chemistry at the C_{60}-ligand heterointerface for hydrogen evolution reactions has not been completely unveiled.

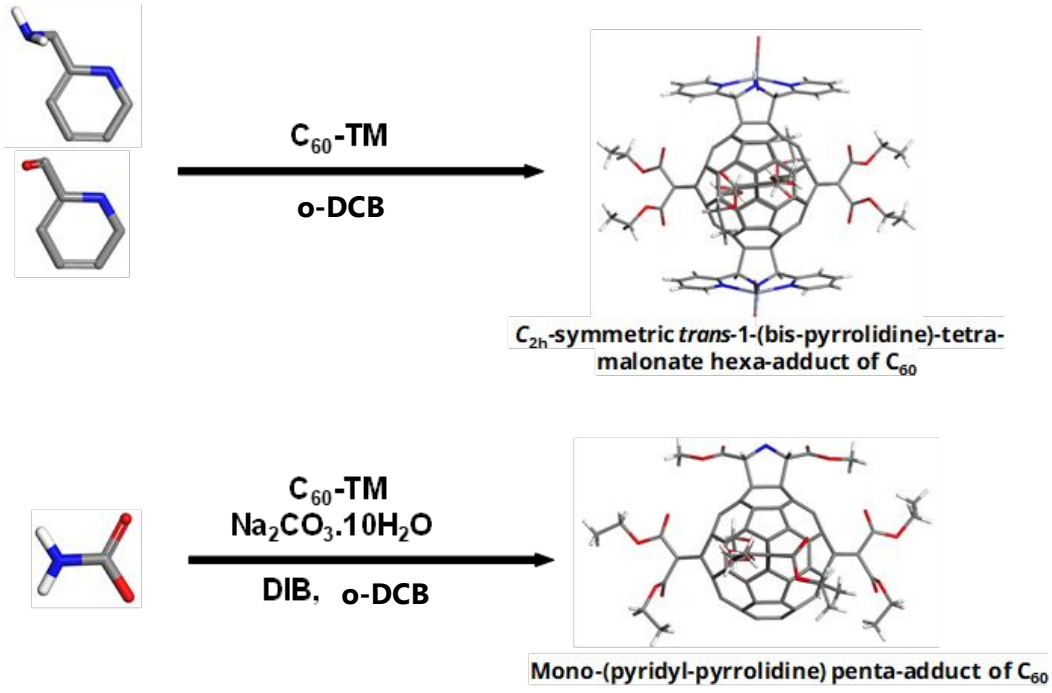

Figure 1. Synthesis of penta and hexa-adducts of C_{60}: Hexa-adduct (C_{2h}-Symmetric trans-1-(Bis-pyrrolidine)-tetra-malonate Hexa-Adducts of C_{60}) and penta-adduct-C_{60} (mono-pyrrolidine penta-adduct of C_{60}) were synthesized through the reaction of C_{60}-TM with methyl glycine ester, using diacetoxyiodobenzene (DIB) and sodium carbonate decahydrate as reagents in ortho-dichlorobenzene (o-DCB), under sonication at room temperature.

In this work, we report an activation approach involving the regio- and stereoselective synthesis of hybrid fullerene C_{60} penta (P-C_{60}) and hexa-adduct (H-C_{60}).[17] These functionalized fullerenes showed an exceptional electron density relocation at the C_{60}-ligand interfaces, which significantly impacts the electronic structure of the carbon atoms in the nearest regions, thus inducing a new type of highly active electrocatalytic sites for the molecular generation of hydrogen. Hexa and Penta adduct of C_{60} are prepared as shown in the scheme presented in **Figure 1 and Supporting Information 1**.

The ^{13}C NMR spectrum **(Figure S1-S3)** of H and P -C_{60} exhibited resonances analogous featuring carbonyl group signals at δ=163.8 and 163.4 ppm, seventeen signals between 156.1 and 122.6 ppm corresponding to twelve sp^2 fullerene carbon atoms and five 2-pyridyl groups, pyrrolidine addend signals at δ=70.6 and 76.5 ppm, methylene group signals at δ=62.7 and 62.1 ppm, and methyl group signals at δ=14.1 ppm. Furthermore, five additional signals at δ=72.7, 70.9, 66.2, 45.4, and 44.1 ppm confirmed the presence of the cis-anti-cis isomer.[18] The crystal data of the as-separated structures of penta and hexa adduct are presented in **(Figure S4 and Supporting Information 2)**. The exclusive formation of cis-anti-cis hexa-adduct isomers was primarily ascribed to the interactions between the pendant groups in the malonate and the pyrrolidine rings. These interactions, crucial in the gas phase (van der Waals forces), are diminished when the solvent (o-DCB) is present.

The hydrogen evolution characteristics of functionalized fullerenes were investigated through linear sweep voltammetry (LSV) in 0.5 M H_2SO_4 **(experimental details in Supporting Information 3)**. Catalytic activities for hydrogen evolution are depicted in **Figure 2A**, showcasing Pristine C_{60}, P-$C_{60,}$ and H-C_{60}, alongside the benchmark Pt/C. The onset potentials and current densities for Hexa and Penta functionalized fullerenes (-90 mV and −45 mV vs. RHE) significantly exceed those of Pristine C_{60}, suggesting that organic functionalization decreases the uphill thermodynamic barrier towards the hydrogen adsorption in the fullerene cage.[17] Notably, the catalytic activity of P-C_{60} surpasses that of the H-C_{60}, reflecting the importance of the group, as well as the degree of functionalization and symmetry.[17] Remarkably, P-C_{60}, with an onset potential of −45 mV vs. RHE, an overpotential of 75 mV to reach 10 $mA \cdot cm^{-2}$ and a high current density of 160 $mA \cdot cm^{-2}$ at −0.6 V vs. RHE, outperforms the HER activity of the state-of-the-art metal-free carbon nanostructure electrocatalysts (**Table S1, Supporting Information 4**). The superior catalytic activity of the P-C_{60} can be associated with the unique distribution of ester-pyrrolidine motif in the carbon cage, which activates the nearest carbon atoms at the C_{60}-ligand interfaces, thus creating new highly active centers, enhancing the adsorption of catalytic intermediates, and improving the catalytic rates for the HER. Tafel plots provide insights into the HER mechanisms of the functionalized C_{60} surfaces, with the Penta-C_{60} adduct displaying a Tafel slope of 48 $mV \cdot dec^{-1}$ (**Figure 2b)**. It is worth pointing out that the Tafel slope of the functionalized C_{60} molecules is by far lower than that of pristine C_{60}, thus implying a more efficient HER pathway, possibly the Volmer–Heyrovsky mechanism, and an improved kinetic efficiency upon the fullerene functionalization.

Furthermore, the P-C_{60} demonstrates remarkable electrochemical stability in acidic conditions, maintaining 97% of the initial current density after 20000s, as evidenced in **Figure S5, Supporting Information 4**. Mott–Schottky (M-S) and diffuse reflectance spectroscopy (Bandgap)

analyses were conducted to assess the charge carrier densities (N_d) for the HER of the electrochemical materials **(Figure 2c and Figure 2d)**.

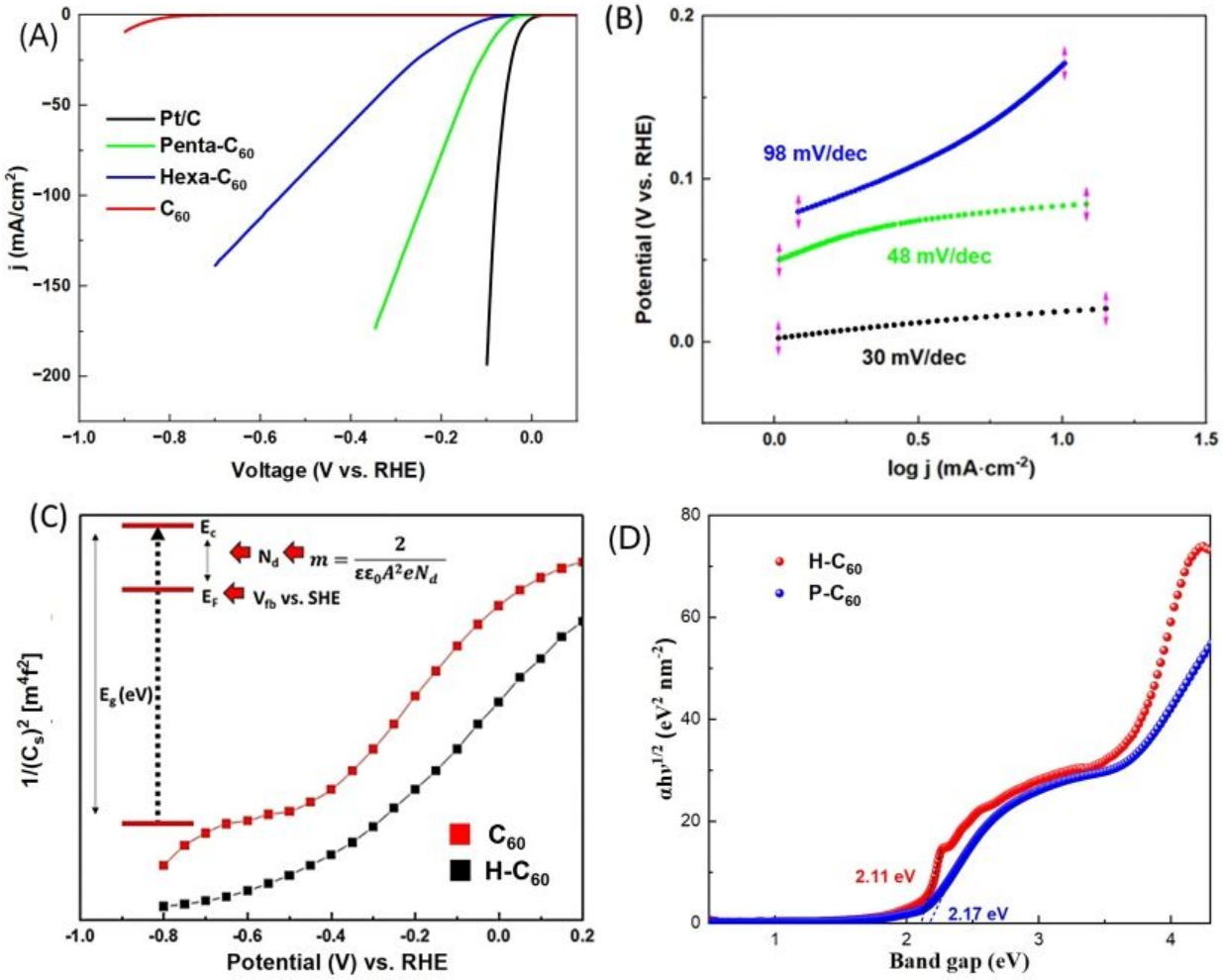

Figure 2. (A) Hydrogen evolution linear sweep voltammetry profile of Pristine C_{60}, Hexa adduct of C_{60}, H- C_{60} and Penta adduct P-C_{60} the benchmark Pt/C. (B) Tafel slope of the optimum Penta adduct C_{60} and Pt/C; (C) Mott-Schottky analysis of C_{60} and H-C_{60}. (D) DRS profile of the Hexa (Red) and Penta (blue) adduct of C_{60}

The well-established inverse relationship between the M-S and N_d suggests that a decrease in slope corresponds to an increase in N_d, thereby enhancing the charge carrier densities and consequently, the electron transfer kinetics. The P-C_{60} exhibited a lower slope than non-functionalized C_{60} fullerenes, suggesting that functionalization improves the charge carriers, significantly boosting the charge transfer at the M-S interfaces. Furthermore, the flat band potential shifted from -0.6 V for pristine C_{60} to -0.4 V for the P-C_{60}, suggesting a higher electron density near the Fermi level in the case of the P-C_{60}. Additionally, XPS experiments were carried out before and after a chronoamperometric experiment with the F-C_{60} **(Figure S6, Supporting Information 5).** Ex-situ XPS after the chronoamperometry experiment shows a slight shift in the N1s band most likely due to the electron transfer processes in the C_{60}-addend interface (**Figure**

S6b). The Faradaic efficiency (FE) of P-C_{60} catalysts was also determined by dividing the measured H_2 produced by the expected amount based on the charge passed during controlled-potential electrolysis measurements. For longer 24-hour experiments, the FE was found to be 89%, a promising value for a metal-free HER catalyst.[20] **(see Table S2, Supporting Information 5).**

To unlock the effects of the ligand functionalization strategy in the HER electrocatalytic properties of C_{60} fullerenes and gain an in-depth mechanistic understanding, we employed Density Functional Theory (DFT) calculations. We first calculated the electronic properties of H-C_{60} and P-C_{60} adducts. The density of states of the H-C_{60} and P-C_{60} molecules was studied using different link groups **(Figure 3a and Figure 3d)**. For the H-C_{60} adduct, the group-1 has a higher contribution to the C_{60} compared to the group-2 **(Figure 3a)**. The density of states near the Fermi level was mainly contributed by the 2*p* orbitals of C and N atoms **(Figure 3g)**. Moreover, the 2*p* orbital of O atoms from the addends is hybridized with the 2*p* orbital of C atoms in the cage, indicating that the addends exhibit a strong interaction with the C_{60} cage. The P-C_{60} adduct shows the same trend **(Figure 3d and Figure 3h)**.

We further calculated the charge distribution of the H-C_{60} and P-C_{60} to uncover the charge change of the C atoms at the C_{60}-addend interfaces. The calculated Bader analysis shows that there are significant electron transfers between the ligands and C_{60} atoms. Depending on the distance from the functional group, the C atoms of C_{60} will gain or lose different electrons. For the P-C_{60}, the first nearest C atoms that are directly connected to the functional group will gain 0.02~0.12 electrons from the functional groups. The second nearest C atoms may gain or lose electrons according to their distance from the other functional groups. For H-C_{60}, the first nearest C atoms that are directly connected to the functional group lose 0.08 electrons while the second nearest C atoms all gain 0.01~0.3 electrons. The C atoms of pristine C_{60} are not active for HER due to the weak interaction with the H.[19]

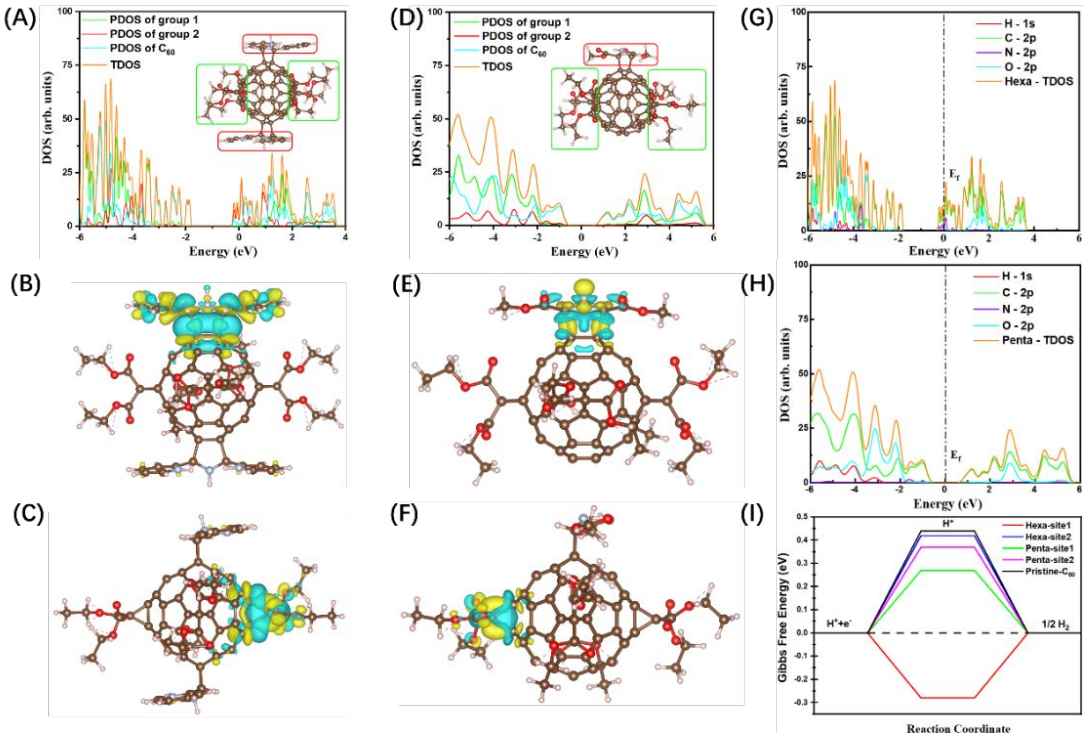

Figure 3. The calculated density of states and charge density difference maps of different ligands for H-C_{60} (A), (B) (C) and P-C_{60} (D), (E) (F); the calculated density of states for different elements contribution of H-C_{60} (G) and P-C_{60} (H); (I)the calculated Gibbs free energies for different C sites of H-C_{60} and Penta-C_{60}, the pristine C_{60} was included for comparison (the iso-surface value is 0.0015 e $Å^{-3}$).

After the functionalization, the electronic properties of C atoms that are near the addends were drastically affected. There are two different types of addends for the H-C_{60} and P-C_{60} adducts (pyridine and ethyl ester groups, respectively). We have calculated the charge density difference maps of H-C_{60} and P-C_{60} for each type of addend, respectively. There is a charge transfer process from the ligands to the C atoms of the C_{60} cages **(Figure 3b, Figure 3c, Figure 3e and Figure 3f)**. The calculated Bader analysis shows that the ligands release electrons and the C atoms near the ligands gain electrons, thus promoting an intramolecular electron transfer phenomenon. Moreover, the charge distribution of C atoms around the functional groups on the C_{60} cage can also influence the H absorption strength during the electrocatalytic reaction. To verify this prediction, the Gibbs free energy values of the absorbed H on different C sites were calculated. As expected, the ideal HER catalyst requires a value of ΔG_{H^*} close to zero. According to the distance between the C atoms of C_{60} and the ligands, two types of catalytic sites, including the first and second nearest C atoms, were investigated **(Figure S7 and Figure S8, Supporting Information 6).** The results show that the first nearest C atoms were the most active sites for HER with Gibbs free energies of -0.28 and 0.27 eV for H-C_{60} and P-C_{60}, respectively. As the distance between the C atoms and ligands increases, the Gibbs free energy of the absorbed H becomes more positive (0.42 and 0.37 eV for H-C_{60} and P-C_{60}, which is close to the 0.44 eV of pristine C_{60}), suggesting a substantial change in the HER efficiency **(Figure 3i)**.
In summary, we have disclosed the principal factors that control the intermolecular electron transfer at the C_{60}-addend interface and their implication for the molecular generation of hydrogen. The C_{60}-addend interface can finely tailor the nearest carbon atoms' electronic structure and decrease the H adsorption's thermodynamic barrier, thus promoting the overall catalytic activity. We have also proven the importance of the pyrrolidine addends, being more active in the ester groups when compared with those from the pyridine. This work offers a unique approach to the rational design of functionalized fullerene-based molecular catalysts for efficient electrochemical hydrogen evolution.

Acknowledgements
MN acknowledges the financial support provided by the Partnership for Research and Education in Materials (PREM) by the U.S. National Science Foundation (NSF) (NSF PREM: Award # 1827820). MN acknowledges the financial support from the new investigator award (Virginia Space Center and NASA). CD acknowledges the financial support provided by the U.S. Department of Energy, Office of Science, Office of Basic Energy Sciences, Heavy Element Chemistry program under Award Number DE-SC0023050.

Corresponding Authors

Mohamed Noufal
Hampton University
mohamed.noufal@hamptonu.edu
Tianwei He
Yunnan University
he.tianwei@ynu.edu.cn
Alain Rafael Puente Santiago
Florida International University
alpuente@fiu.edu

Declaration of Competing Interest

The authors declare that they have no known competing financial interests or personal relationships that could have appeared to influence the work reported in this paper.

Additional Information

Crystallographic information and ^{1}H- and ^{13}C-NMR spectra for P-C_{60} and H-C_{60}.

References

1. X. Cui, M. Wu, X. Liu, B. He, Y. Zhu, Y. Jiang and Y. Yang, *Chem. Soc. Rev.*, 2024, **53**, 1447-1494..
2. D. Zhang, Z. Wang, F. Liu, P. Yi, L. Peng, Y. Chen, L. Wei and H. Li, *J. Am. Chem. Soc.*, 2024, **146**, 3210-3219.
3. A. R. Puente Santiago, M. F. Sanad, A. Moreno-Vicente, M. A. Ahsan, M. R. Cerón, Y.-R. Yao, S. T. Sreenivasan, A. Rodriguez-Fortea, J. M. Poblet and L. Echegoyen, *J. Am. Chem. Soc.*, 2021, **143**, 6037-6042.
4. J. Durst, A. Siebel, C. Simon, F. Hasché, J. Herranz and H. A. Gasteiger, *Energy Environ. Sci.*, 2014, **7**, 2255-2260.
5. Y. Lu, L. Tang, P. Wang, M. He, C. Yang and Z. Li, *ACS Catal.*, 2023, **13**, 13804-13815.
6. Z. Jiang, W. Zhou, A. Hong, M. Guo, X. Luo and C. Yuan, *ACS Energy Lett.*, 2019, **4**, 2830-2835.
7. H. Huang, M. Yan, C. Yang, H. He, Q. Jiang, L. Yang, Z. Lu, Z. Sun, X. Xu, Y. Bando and Y. Yamauchi, *Adv. Mater.*, 2019, **31**, 1903415.
8. S. Pal, M. Sahoo, V. T. Veettil, K. K. Tadi, A. Ghosh, P. Satyam, R. K. Biroju, P. M. Ajayan, S. K. Nayak and T. N. Narayanan, *ACS Catal.*, 2017, **7**, 2676-2684.
9. M. Batabyal, S. Jaiswal, R. K. Jha and S. Kumar, *J. Am. Chem. Soc.*, 2024, **146**, 57-61.
10. A. A. Feidenhans'l, Y. N. Regmi, C. Wei, D. Xia, J. Kibsgaard and L. A. King, *Chem. Rev.*, 2024, **124**, 5617-5667.
11. K. Muñoz-Becerra, F. J. Recio, R. Venegas and J. H. Zagal, *Curr. Opin. Electrochem.*, 2023, **42**, 101387.
12. A. R. Puente Santiago, T. He, O. Eraso, M. A. Ahsan, A. N. Nair, V. S. N. Chava, T. Zheng, S. Pilla, O. Fernandez-Delgado, A. Du, S. T. Sreenivasan and L. Echegoyen, *J. Am. Chem. Soc.*, 2020, **142**, 17923-17927.
13. L. Song, T. Li and S. Zhang, *J. Phys. Chem. C*, 2017, **121**, 293-299.
14. A. C. Bevilacqua, M. H. Köhler and P. C. Piquini, *J. Phys. Chem. C*, 2019, **123**, 20869-20876.

15. M. F. Sanad, H. M. Franklin, B. A. Ali, A. R. Puente Santiago, A. N. Nair, V. S. N. Chava, O. Fernandez-Delgado, N. K. Allam, S. Stevenson, S. T. Sreenivasan and L. Echegoyen, *Angew. Chem. In. Ed.*, 2022, **61**, e202116727.
16. W. Yang, Q. Huang, Y. Yan, Y. Li, T. Xu, A. Yu, Y. Zhao, P. Peng, Y. Wang, L. Echegoyen and F.-F. Li, *Angew. Chem. In. Ed.*,2024, e202414149.
17. E. Castro, K. Azmani, A. H. Garcia, A. Aghabali, S. Liu, A. J. Metta-Magana, M. M. Olmstead, A. Rodríguez-Fortea, J. M. Poblet and L. Echegoyen, *Chem .Eur. J.*, 2017, **23**, 15937-15944.
18. E. Castro, K. Azmani, A. H. Garcia, A. Aghabali, S. Liu, A. J. Metta-Magana, M. M. Olmstead, A. Rodríguez-Fortea, J. M. Poblet and L. Echegoyen, *Chem. Eur. J.*, 2017, **23**, 15841-15841.
19. T. He, G. Gao, L. Kou, G. Will and A. Du, *J. Catal.*, 2017, **354**, 231-235.
20. M. Cai , L. Xu , J. Guo , X. Yang , X. He and P. Hu , *J. Mater. Chem. A*, 2024, **12** , 592-612 .

Data availability

The authors confirm that the data supporting the findings of this work is available within the article and its Supporting Information. The raw data is also accessible from the corresponding author upon reasonable request.